Effect of temperature on hydrogen embrittlement susceptibility of alloy 718 in Light Water Reactor environment

Florian Galliano, Eric Andrieu, Jean-Marc Cloué, Grégory Odemer, Christine Blanc

Effect of temperature on hydrogen embrittlement susceptibility of alloy 718 in Light Water Reactor environment

Florian Galliano [a], *Eric Andrieu* [b], *Jean-Marc Cloué* [c], *Gregory Odemer* [b,*], *Christine Blanc* [b]

[a] *MBDA, Avenue D'Issoudun, 18000 Bourges, France*
[b] *CIRIMAT, Université de Toulouse, CNRS, INPT, UPS, ENSIACET, 4 Allée Emile Monso, BP 44362, 31030 Toulouse Cedex 4, France*
[c] *Spinodal Conseil, 3 Rue Louis Lumières, 31300 Toulouse, France*

ARTICLE INFO

Keywords:
Nickel alloys
Hydrogen embrittlement
Fracture modes

ABSTRACT

A 718 superalloy, presenting a standard microstructure, was mechanically tested under uniaxial tensile loading at 80 °C and 300 °C in Light Water Reactor environment after an exposure at 300 °C for 200 h. Hydrogen embrittlement mechanism was clearly observed. In order to identify the most influent metallurgical parameters on hydrogen embrittlement, three "model" microstructures were synthesized to test the efficiency of carbides, δ, γ′ and γ" precipitates to trap hydrogen at different temperatures. Results showed that γ′ and γ" played the major role on the hydrogen embrittlement susceptibility of the alloy even though carbides and δ precipitates could also act as hydrogen traps and influence the final rupture mechanism. Results also characterized the influence of temperature on the fracture modes.

Introduction

Alloy 718 is a Ni based superalloy used in Light Water Reactor (LWR) environments for structural components. It is strengthened by precipitation of stable γ′ (Ni_3(Ti,Al)) and metastable γ″ (Ni_3Nb) precipitates [1]. Because of fabrication processes, the precipitation of the stable form of γ″, i.e. δ phase, may occur [2]. In operating conditions, alloy 718 is exposed to high temperature (300 °C) and pressure (150 bars) in primary water environment. In these conditions, corrosion processes occur at the surface of the material and cause hydrogen absorption in alloy 718 [3].

The presence of hydrogen in Ni based alloys and particularly in alloy 718 can cause brittle fracture under a mechanical loading [4–16]. Several studies reported hydrogen embrittlement (HE) for specimens mechanically loaded at relatively low temperature (below 150 °C) [7–11] but Fukuyama et al. [12] and Wei et al. [13] showed that alloy 718 tested at 300 °C and 600 °C under gaseous hydrogen conditions could present a surprising

* *Corresponding author.*
E mail address: gregory.odemer@ensiacet.fr (G. Odemer).
http://dx.doi.org/10.1016/j.ijhydene.2017.06.211

reduction of elongation to failure compared to tests performed under air conditions despite a ductile fracture. Nevertheless, there are only few studies focused on the effect of corrosion induced HE in alloy 718 at high temperature.

Other authors explored the role of precipitates in the mechanism of HE in alloy 718 at lower temperatures [14–17], such as room temperature. Liu et al. [14] showed that hydrogen induced cracking in δ rich alloy 718 occurred at δ/ matrix interfaces. In addition, the presence of δ intragranular precipitates promoted the occurrence of transgranular cracks [15]. Furthermore, hydrogen diffusivity and solubility were also affected by the presence of precipitates in alloy 718 [18]. At higher temperatures, dislocations, primary carbides, γ′, γ″ and δ precipitates are often considered as potential hydrogen traps [5,14–16].

In the present study, the effects of corrosion induced HE of alloy 718 were studied at 80 °C and 300 °C by means of slow strain rate tensile tests at 1.10 ^{5} s ^{1} performed in autoclave after exposure at 300 °C in primary water environment. Additionally, tensile tests were conducted in air on "model" microstructures of alloy 718 with a controlled metallurgical state. These "model" microstructures were hydrogen precharged before tensile tests in order to better understand the results obtained for alloy 718 and draw conclusions on the influence of hydrogen traps on HE susceptibility and me chanical behavior of this alloy.

Material and experimental procedure

Material

Standard composition of alloy 718 is reported in Table 1. Flat tensile samples (ISO 6892 2:2011) of alloy 718 were tested in LWR environment (samples called A in Table 2). They were machined along the rolling direction from 6 mm thick plates, which had been previously cold worked at 11.5%. They were then mechanically grinded to 1.5 mm and submitted to a standard ageing (SA) heat treatment. This treatment consisted of a dwell of 8 h at 720 °C, then cooling at 50 °C/h and a final dwell at 620 °C during 8 h. It allowed precipitation of γ′ and γ″ phases [1]. After heat treatment, metallographic observations were carried out confirming the presence of γ′ and γ″ pre cipitates. Small δ phase precipitates were also observed, their precipitation having been enhanced by cold working process (Fig. 1a). Grain size was determined to be ASTM 8 9.

Since all the previously cited precipitates and defects may act as hydrogen traps, three "model" microstructures were synthesized to distinguish the influence of each type of pre cipitates on the HE susceptibility of alloy 718. The "model" microstructures were obtained from samples machined in 0.5 mm thick sheet of alloy 718 that had been previously so lution annealed. Table 2 presents thermo mechanical fabrication process and expected hydrogen traps for each metallurgical state. Samples B were not submitted to an additional heat treatment after being removed from the sheet and only presented carbide precipitates (Fig. 1b). Metallurgical state C was obtained by performing a standard ageing treat ment on the sheet inducing precipitation of nano scaled γ′ and γ″ precipitates without any δ phase (Fig. 1c). Finally, samples D were heat treated at 960 °C for 48 h before being submitted to the standard ageing in order to precipitate large δ platelets and globular δ precipitates (Fig. 1d) in addition to γ′ and γ″. B, C and D samples presented a homogeneous grain size of ASTM 9 10. All the microscopic observations of these microstructures have already been presented in detail in a previous work [19]. For all samples, surface preparation before experimental tests was realized using a 1200 grid SiC paper.

Hydrogen charging processes and mechanical tests

Hydrogen charging was conducted in primary water envi ronment for samples presenting metallurgical state A. They were exposed during 200 h in a static autoclave. Primary water consisted of pure water with addition of 1200 ppm B (weight) as H_3BO_3 and 2 ppm Li (weight) as LiOH. The temperature of the exposure was fixed at 300 °C under a pressure of 125 bar. An addition of ArH_2 was carried out in order to control the partial pressure in hydrogen. At 300 °C, it was estimated to be close to 0.3 bar.

After 200 h of exposure, the autoclave was stabilized or cooled to reach the tensile test temperature. Two tempera tures were explored, 80 °C and 300 °C, and tensile tests were conducted until fracture occurred. The strain rate during tensile tests was fixed at 1.10 ^{5} s ^{1} whatever the testing temperature. The tensile line was equipped out of the auto clave with a Linear Variable Differential Transformer and the driving source was a stepper motor using a controller with load feedback.

In order to test various metallurgical states, additional experiments were performed on "model" microstructures using cathodic hydrogen charging process followed by me chanical tests in air. Hydrogen charging was performed during 4 h in a molten salt bath (53.5 wt % $NaHSO_4$, H_2O 46.5 wt % $KHSO_4$) at 150 °C with an applied potential of 1000 mV versus a silver electrode. This technic was described in detail in a previous work [20]. Samples B, C and D were then maintained in a furnace at 300 °C for 30 min for desorption and H content homogenization, before being tested [19]. This allowed to avoid potential effects of diffusible hydrogen on mechanical properties coupled to its desorption/redistribution during the tensile tests. Mechanical tests were conducted on these samples at 300 °C on a tensile machine outfitted with an environmental furnace and a non contacting laser exten someter to measure the strain of the samples. The strain rate was fixed at 1.10 ^{5} s ^{1}. Mechanical properties of H free and H

Table 1 – Standard chemical composition of alloy 718 (wt %).

	Fe	Ni	Cr	Nb + Ta	Mo	Ti	Al	Mn	Si	Co	C	P	S
Min	Bal.	50	17	4.75	2.8	0.65	0.2						
Max	Bal.	55	21	5.5	3.3	1.15	0.8	0.35	0.35	0.1	0.08	0.015	0.015

Table 2 – Metallurgical state of alloy 718, heat treatments and testing conditions.				
Metallurgical states	Thermomechanical treatments	Expected hydrogen traps	Hydrogen charging conditions	Testing conditions
A	Solution annealed Cold worked 11.5% SA	Dislocations, γ′, γ″, few δ, carbides	LWR environment	LWR environment
B	Solution annealed	Carbides (volume fraction = 0.2%)	Molten salt bath 150 °C	Air
C	Solution annealed SA	γ′, γ″, carbides (volume fraction of γ′ γ″ = 17%)	Molten salt bath 150 °C	Air
D	Solution annealed 960 °C/48 h SA	γ′, γ″, large δ, carbides (volume fraction of γ′ γ″ = 12%; volume fraction of δ = 5%)	Molten salt bath 150 °C	Air

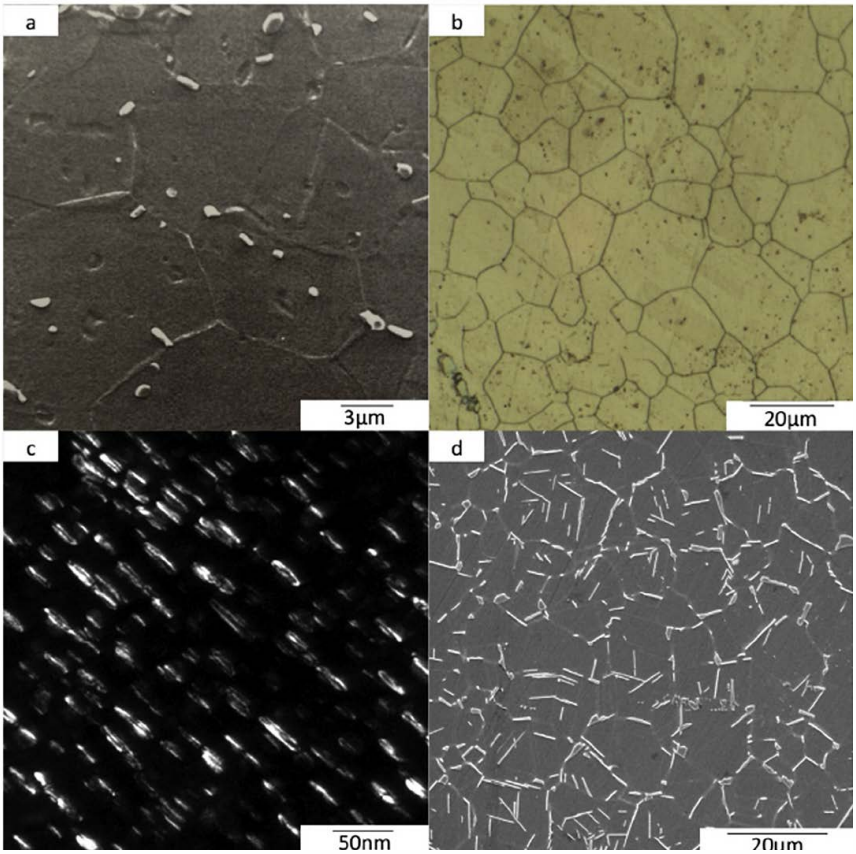

Fig. 1 – Microstructural observations of: (a) Metallurgical state A - SEM, (b) Metallurgical state B - Optical Microscope, (c) Metallurgical state C - TEM, (d) Metallurgical state D – SEM.

exposed samples were determined after tensile tests. From these results, HE was followed by using an embrittlement factor EF [8] based on the loss of elongation because of the presence of hydrogen in the material:

$$EF \quad (\varepsilon_0 \quad \varepsilon_H)/\varepsilon_0 \qquad (1)$$

where ε_0 and ε_H represented the plastic elongation to failure measured at the same temperature on H free sample tested in air and H exposed specimen (to LWR environment or charged by cathodic method) respectively. After failure, fracture surfaces were observed by means of a Scanning Electron Microscope (LEO 435VP SEM).

Global hydrogen content was measured using a Galileo Bruker analyzer. Hydrogen was extracted by the fusion (1550 °C) of each sample in inert gas (Argon) and analyzed by a high sensitivity thermal conductivity detector just after cathodic charging. Hydrogen content was assumed to be uniform all along a plane parallel to the charging side. A gradient in the direction perpendicular to the charging side might exist despite of the homogenization treatment previously described for samples B, C and D.

Results and discussion

Hydrogen embrittlement after exposure in LWR environment

Mechanical properties determined for healthy A samples in air or for A samples after exposure and tensile tests in LWR

environment are presented in Table 3. The Yield Strength (YS) and Ultimate Tensile Strength (UTS) evaluated on the basis of 3 tests performed for each condition were not strongly affected by the testing temperature (80 °C or 300 °C) suggesting that the temperature in the tested range has no significant influence on the behavior law of this metallurgical state. This remark could be drawn for both H precharged and uncharged specimens. In addition, the presence of hydrogen did not seem to affect YS, UTS and work hardening for all explored testing temperatures. On the contrary, the elongation to fail ure of uncharged samples and of hydrogen precharged spec imens slightly decreased when testing temperature increased. It was of 13% at 80 °C but only 10% at 300 °C for uncharged samples. But, the major result was that the elongation to failure seemed highly affected by the presence of hydrogen before testing whatever the temperature. Indeed it was only of 9% at 80 °C and 7% at 300 °C for H precharged samples. As a consequence, EF was relatively high with a value of approxi mately 30% whatever the temperature. These values (31% and 27% at 80 and 300 °C respectively) are in good agreement with results provided for Ni Based alloys [6–8] at lower tempera tures but similar strain rates. However, only few papers report an effect of hydrogen on ductility at high temperatures [12,13].

To deepen mechanical properties analysis, fracture surface observations were carried out. All uncharged samples tested at 80 °C or 300 °C presented a ductile fracture with dimples. On the contrary, samples tested at 80 °C after exposure in primary water exhibited a mixed brittle and ductile fracture (Fig. 2a). Brittle fracture appeared to be mostly transgranular with the presence of cleavage facets (Fig. 2a). These results are in good agreement with those obtained at room temperature on H charged samples in gaseous atmosphere or by cathodic charging methods [8,14]. For hydrogen charged samples tested at 300 °C in LWR environment, a ductile fracture with dimples was observed (Fig. 2b). Nevertheless, it appeared that dimple size was very small, roughly a few nanometers, regarding to uncharged samples. These small dimples were located on what seemed to be a former grain facet. This has been already suggested by Wei [13] and Liu [14] and was attributed to both γ′, γ″ precipitates and carbides.

It is worth noticing that a similar hydrogen EF can then be related either to a macroscopic brittle fracture (at 80 °C) or to a ductile fracture (at 300 °C). Ductile fracture appeared also affected by the presence of hydrogen with an important loss in ductility, suggesting that the presence of hydrogen could weaken precipitates/matrix interfaces. Several in terpretations of this phenomenon consider that precipitates act as brittle inclusions on which dimples are initiated easily [19,20]. Although these precipitates were regularly distributed in the matrix, the localization of slip bands in [111] planes [21,22] led to the coalescence of the cavities and enhanced a localized transgranular ductile fracture. This result, supported by the aspect of the fracture surfaces, confirmed a modifica tion of hydrogen embrittlement mechanism at 300 °C compared to 80 °C. Numerous studies conducted on different Ni based alloys suggested a potential influence of the various metallurgical traps that can be found in alloy 718, i.e. dislo cations [4,5], carbides [23], δ [14,15], γ′ and γ″ [11–13,16] precipitates.

The differences in fracture mechanisms at 80 °C compared to 300 °C might be attributed to the nature and the efficiency of hydrogen traps. While cooling alloy 718 samples, hydrogen traps could become active whereas they were free of hydrogen at higher temperature. The problem in this case was that metallurgical state of studied alloy 718 was rather complex. It has been previously mentioned that it presented both dislo cations from cold work, δ precipitates, γ′ and γ″ phases and also carbides. Therefore, it is not possible to conclude on the first order trap(s) that led to a loss in ductility and a decrease in dimple size on fracture surfaces of H charged samples tested at 300 °C. Another potential interaction between hydrogen in the lattice and vacancies should be considered. Indeed, interaction of hydrogen with a vacancy in nickel was inves tigated by Tanguy et al. [24] by means of DFT calculations. They showed that the absolute vacancy concentration, at room temperature, was enriched of 10 orders of magnitude

Table 3 – Mechanical properties of uncharged A specimens tested in air and hydrogen-precharged A specimens tested in LWR environment at 80 °C and 300 °C at 1.10 ^{5} s ^{1}.

Metallurgical state	Tensile test temperature	Uncharged specimens			Hydrogen precharged specimen			
		YS (MPa)	UTS (MPa)	$\varepsilon_{H\text{-}Free}$	YS (MPa)	UTS (MPa)	ε_{H}	EF
A	80 °C	1440	1520	13%	1450	1520	9%	31%
	300 °C	1380	1480	10%	1350	1450	7%	27%

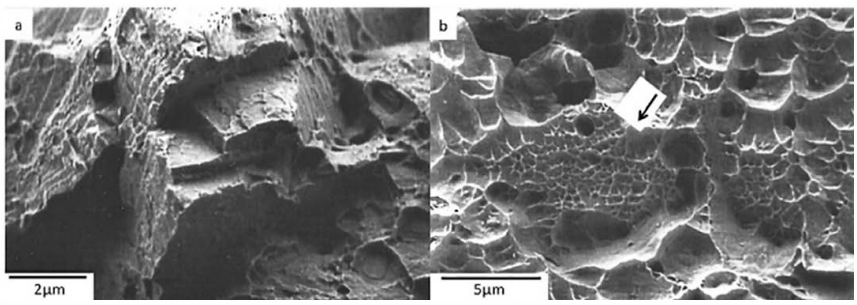

Fig. 2 – Fracture surface of samples exposed and tested in LWR environment at (a) 80 °C, (b) 300 °C.

with respect to thermal vacancies, for hydrogen content of 1000 ppm, leading to HE. In comparison, the average hydrogen concentration in a LWR environment around 300 °C, in the presence of active stress corrosion cracks (i.e. frequent depassivation/repassivation events) was roughly 40 ppm. In LWR conditions, it seems that hydrogen should not have noticeable effects. Nevertheless, the difficulty to determine experimentally the local hydrogen concentration on samples oxidized in well controlled condition in the nanometer scale process zone of a stress corrosion crack, did not preclude a potential superabundant vacancies phenomenon.

Other authors studied the interactions between hydrogen vacancy complexes and dislocations by using multi scale simulation techniques [25,26]. They highlighted the role of hydrogen vacancy complexes on nano voids formation due to dislocation plasticity in α Fe during HE. The concentration of hydrogen vacancy complexes can reach extremely high levels during dislocation plasticity in the presence of hydrogen, and these hydrogen vacancy complexes prefer to aggregate by absorbing additional vacancies and act as nuclei for nano voids. Moreover, they showed that, when approaching a vacancy H complex, the edge dislocation was first attracted and in most cases pinned by the complex. The pinning strength of a vacancy H complex or cluster on the edge dislocation increased with the increasing number of hydrogen atoms trapped in vacancy or vacancy cluster. This inherent pinning mechanism mainly due to the migration of hydrogen atoms in vacancy or vacancy cluster when it was cut by the moving edge dislocation could influence the hydrogen induced deformation and failure and finally HE. Finally Li et al. [25] have shown that the nano voids formation due to hydrogen vacancy complexes resulted in the observation of nano dimples on fracture surfaces that could be related to the nano ductility observed on the samples tested at 300 °C in this paper. Also this similarity suggested that, in the present work, this phenomenon was operative only during finale rupture, maybe for a critical strain level, since only the elongation to failure was modified by hydrogen during tensile tests. A recent work of Lawrence et al. suggested that hydrogen enhanced vacancy clustering could induce an Orowan type hardening component, which is effective even when hydrogen is essentially immobile (at low temperature) and that mobile hydrogen (at high temperature) provided an additional hard ening increase by interacting with mobile dislocations to restrict dislocation cross slip [27]. Obviously, these specula tions are not available in the present work given that yield strength and work hardening are not affected by hydrogen.

Assuming that dislocations did not act as hydrogen traps above 250 °C in Ni based alloys [4,5], attention had to be paid to the different behavior of each type of precipitates. There fore, the mechanical behavior of three metallurgical states B, C and D presenting various types of precipitates was studied in air (Table 2).

Influence of carbides and δ phase on hydrogen induced fracture mode at 300 °C

In order to identify the critical influence of δ phase and car bides, the HE susceptibility of B and D metallurgical states was compared to that of samples A. Table 4 presents the mechanical properties and EF measured for these samples. It appeared that hydrogen did not affect the behavior law of solution annealed alloy 718 (sample B) for mechanical tests performed at 300 °C. EF was low with a value of only 2.5%. In addition, fracture surface remained totally ductile with large dimples due to primary carbides.

As previously mentioned, samples B corresponded to solution annealed alloy 718 and only contained primary car bides. In literature [21], carbides are often presented as deep hydrogen traps, which remain active at high temperatures such as 300 °C. Therefore, carbides may be responsible for the major part of hydrogen trapping at these temperatures. Re sults obtained on samples B for alloy 718 showed that, even though carbides could be still efficient as hydrogen traps at 300 °C, they probably did not act significantly on fracture mode and HE mechanisms in this case. This could be explained by the very low ratio of carbides in the studied alloy 718, below 0.6%, regarding precipitation of γ′, γ″ or δ phases.

Samples with precipitation of large δ phase (D metallur gical state) were also tested at 300 °C. Once again the results revealed that hydrogen did not affect the behavior law. Nevertheless, elongation to failure decreased from 26% for H free alloy 718 to 22% for H cathodically precharged samples. The EF was equal to 15%, twice less than for H charged sam ples A tested in LWR environment. For both uncharged and H cathodically precharged samples D, fracture surfaces appeared totally ductile with large dimples. Nevertheless, on H charged samples, δ precipitates were observed in the bot tom of dimples (Fig. 3).

The presence of δ precipitates in the bottom of dimples of alloy 718 mechanically tested at 300 °C was also observed by Fukuyama [12]. This result suggested that δ phases could act as hydrogen traps at high temperatures. Hydrogen located at δ/ matrix interfaces weakened this interface and caused a pre mature initiation of dimples around δ precipitates and there fore a loss of elongation. Nevertheless, since no δ precipitate has been observed in the bottom of dimples for samples A tested in LWR environment, it could be assumed that δ pre cipitates did not act as a first order parameter for HE of samples A. For these samples, HE would be mainly explained by hydrogen trapping on γ′ and γ″/matrix interfaces.

Influence of γ′ and γ″ precipitates on fracture mode at 300 °C

To better understand the influence of γ′ and γ″ precipitates on the properties of alloy 718, C samples were also studied. These specimens were heat treated in order to present only γ′ and γ″ precipitates in addition of primary carbides. As for B and D samples, mechanical tests at 300 °C were conducted for both H free and H cathodically charged C samples (Table 4).

At first, hydrogen content measurements revealed an in fluence of the metallurgical state on hydrogen solubility. As a matter of fact, the precipitation of γ′ γ″ and δ precipitates in duces a decrease in hydrogen solubility in alloy 718. This result can be explained by the combination of two factors. The first is based on the low solubility of hydrogen in γ″ and δ precipitates at the temperatures used and on the volume in which hydrogen can be dissolved, which is reduced by the volume ratio of precipitates [28]. This phenomenon is magnified by the fact that, for the C and D metallurgical states,

Table 4 – Mechanical properties measured in air for uncharged B, C and D specimens and cathodically hydrogen precharged B, C and D samples at 1.10 ^{5} s ^{1}.

Metallurgical states	Tensile test temperature	Uncharged specimens			Hydrogen precharged specimen				Hydrogen content (wt. ppm)
		YS (MPa)	UTS (MPa)	$\varepsilon_{H\text{-}Free}$	YS (MPa)	UTS (MPa)	ε_H	EF	
B	300 °C	420	850	43%	420	850	42%	2.5%	230
C	80 °C	1280	1440	16%	1290	1480	12.5%	22%	58
	300 °C	1200	1350	15%	1150	1280	12%	20%	
D	300 °C	700	1100	26%	700	1100	22%	15%	60

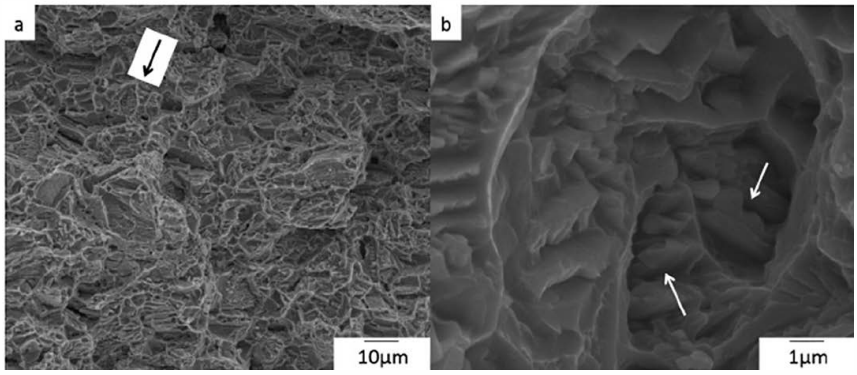

Fig. 3 – Fracture surface of H-charged D samples tested at 300 °C: (a) macroscopic view, (b) magnification of the area marked by the black arrow – white arrows point to δ precipitates.

the majority of Nb and Ti is tied up in the age hardening precipitates. However, in the B material, these elements are dissolved in the matrix, where they may exert their maximum effect in promoting the dissolution of hydrogen in the matrix. Tensile tests showed that mechanical properties were almost comparable with only a slight decrease of YS and UTS when samples were hydrogen precharged. Elongation to failure decreased from 15% to 12% in presence of hydrogen. The value of EF was 20% that was slightly below but comparable to EF measured in LWR environment (27%) for A samples. For C samples, fracture surface observations revealed a ductile fracture with large dimples without hydrogen whereas dimples were very small in presence of hydrogen (Fig. 4). This was consistent with the observations carried out for A samples, tested at 300 °C after exposure in LWR environment.

The presence of small dimples on hydrogen precharged samples presenting γ′ and γ″ precipitates tested at high temperatures was already reported by Wei [13]. He explained that ductile fracture and small dimples could be related to the precipitation of γ′ and γ″ precipitates.

In order to emphasize the influence of γ′ and γ″ precipitates, further mechanical tests were conducted at 300 °C, but with a higher strain rate (5.10 ^{2} s ^{1}) for C samples. This aimed to promote strain localization around γ′ and γ″ precipitates [16,19]. For this strain rate, fracture surface of H precharged samples exhibited several areas with nano scaled dimples that were not observed on H free samples. Pattern and size of these dimples (Fig. 4b) were in good agreement with those of γ′ and γ″ precipitates. Furthermore, precipitates could be seen at the bottom of some dimples; nevertheless, their size (about 30 nm) was too small to allow a good observation or chemical analysis. These results suggested that small γ′ and γ″ precipitates acted in the same way of large δ precipitates despite the fact that YS of D metallurgical state was significantly lower than C metallurgical state. This result could signify that the stress level inducing decohesion of δ/matrix interfaces was lower than the stress level inducing decohesion of γ′ and γ″/matrix interfaces and that the localization of the deformation by dislocation pile up on δ precipitates is sufficient in this case to induce dimple formation.

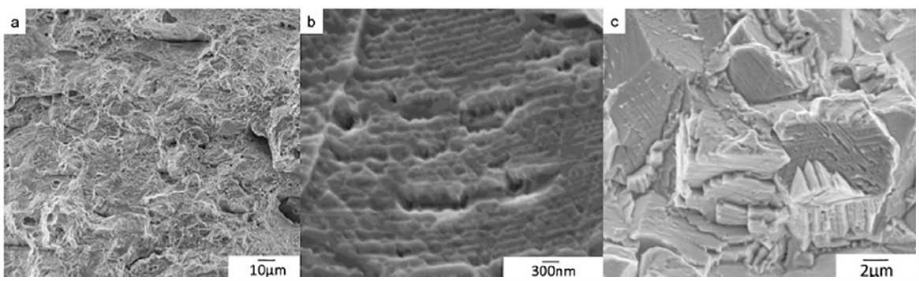

Fig. 4 – Fracture surface for H-charged C samples tested at 300 °C at (a) 1.10 ^{5} s ^{1}, (b) 5.10 ^{2} s ^{1} and (c) tested at 80 °C after a heat-treatment at 300 °C for 30 min.

As a matter of fact, in presence of hydrogen, γ'/matrix and γ″/matrix interfaces were weakened. During tensile tests at high strain rate, cavities initiated at these interfaces and coalesced to cause a premature ductile failure with nano scaled dimples.

Fracture mode at 300 °C in LWR environment (samples A) suggested that the γ′ and γ″ precipitates played the major role in fracture mechanism for A samples. In addition, even though carbides and δ precipitates could act as hydrogen traps at 300 °C, they did not affect significantly fracture mode for samples A at this temperature. This observation contradicts some results found in the literature which showed that δ precipitates were mainly responsible for HE [29]. This difference could be explained by several parame ters such as temperature and strain rate of tensile tests and hydrogen charging method. Indeed the large diversity of experimental parameters in the cathodic charging method can lead to a strong variability in hydrogen content, distri bution and hydrogen trap saturation. Moreover, the differ ence between the precipitate volume ratios of the different metallurgical states of each study could explain this disagreement.

At 300 °C and under LWR conditions, the effect of hydrogen is only observed during the final rupture and seems to be mainly due to hydrogen trapped at γ′ γ″/matrix interfaces.

Role of hydrogen trapping at 300 °C on HE at 80 °C in air

To confirm the previous results, i.e. the strong influence of γ′ and γ″ precipitates on HE for samples A, additional mechani cal tests were performed on samples C. Hydrogen cathodically precharged C tensile samples were tested at 80 °C after 30 min of desorption at 300 °C. During the heat treatment at 300 °C for 30 min, it was assumed that the most part of hydrogen had desorbed from the matrix and that hydrogen remained trapped around γ′ and γ″ precipitates [19]. Results showed that the presence of hydrogen did not affect YS or UTS whereas there was a significant loss of ductility, of about 22%. It is worth noticing that this value was mostly the same as for samples C tested at 300 °C in air (20%) and com parable to the value obtained for samples A tested in LWR environment at 80 °C (31%). Fracture surface was found to be mainly brittle with a large predominance of transgranular brittle facets (Fig. 4c).

Therefore, the morphology of fracture surface on samples tested in air (Fig. 4c) appeared to be the same as for samples A tested in LWR environment (Fig. 2a). This suggested that hydrogen trapping at high temperatures, around 300 °C, could induce a brittle fracture when the samples were mechanically tested at a lower temperature. Indeed, when temperature was lower, i.e. 80 °C, some hydrogen traps such as dislocations could become more efficient. Therefore, a hydrogen enhanced localized plasticity (HELP) mechanism based on an increase in dislocation mobility by the reduction of the elastic in teractions between obstacles and perfect and/or partial dis locations could be assumed [30]. Associated with a hydrogen transport phenomenon facilitated by dislocations, this mechanism led to local segregation of hydrogen on {111} planes, inducing cleavage, as well as the decohesion of par ticles/matrix interfaces (HID mechanism) [31,32].

In addition, the results evidenced that fracture modes of samples tested at 80 °C in LWR environment after 200 h of exposure to LWR environment could be reproduced by me chanical tests in air performed on hydrogen cathodically charged samples after an appropriate short term heat treatment.

Conclusion

Alloy 718 presenting carbides, δ, γ′ and γ″ precipitates was exposed to LWR environment at 300 °C. It was then mechan ically loaded and exhibited sign of brittle fracture and loss in elongation when the mechanical tests were performed at 80 °C. After mechanical tests at 300 °C, fracture appeared ductile with very small dimples but loss in elongation was still relatively high and comparable to the results obtained at 80 °C. The effect of hydrogen at 300 °C was attributed to the presence of metallurgical traps that were still active at 300 °C and on which ductile fracture, i.e dimples, was initiated.

Comparison of fracture modes and EF obtained after ten sile tests at 300 °C on alloy 718 and for different "model" mi crostructures with controlled metallurgical states helped to identify the most prevalent hydrogen traps on fracture mechanisms. Therefore δ, γ′ and γ″ precipitates clearly appeared to cause a premature ductile failure. For samples presenting both small δ precipitates, carbides, γ′ and γ″ pre cipitates, γ′ and γ″ precipitates seemed to have the major ef fect. Results also showed that hydrogen trapping at high temperatures on metallurgical hydrogen traps could lead to brittle fracture when the temperature for mechanical tests decreased.

Finally, from a macroscopic point of view, since the constitutive laws of all microstructures were not modified by hydrogen, and particularly the yield strength, it can be concluded that hydrogen has no effect on crack initiation step on the surface of smooth tensile specimen. The effect of hydrogen occurred during final fracture and then can be revealed only on fracture surfaces.

REFERENCES

[1] Oblak JM, Paulonis DF, Duvall DS. Coherency strengthening in Ni base alloys hardened by DO_{22} γ'' precipitates. Metall Trans 1974;5:143 53.

[2] Huang Y, Langdon TG. The evolution of delta phase in a superplastic Inconel 718 alloy. J Mater Sci 2007;42:421 7.

[3] Totsuka N, Lunarska E, Cragnolino G, Szklarska Smialowska Z. Effect of hydrogen on the intergranular stress corrosion cracking of alloy 600 in high temperature aqueous environments. Corrosion 1987;43:505 14.

[4] Lecoester F, Chene J, Noel D. Hydrogen Embrittlement of the Ni base Alloy 600 correlated with hydrogen transport by dislocations. Mat Sci Eng A 1999;262:173 83.

[5] Chene J, Brass AM. Role of temperature and strain rate on the hydrogen induced intergranular rupture in alloy 600. Metall Trans A 2004;35:457 64.

[6] Symons DM. The effect of hydrogen on the fracture toughness of alloy X 750 at elevated temperatures. J Nucl Mater 1999;265:225 31.

[7] Hicks PD, Altstetter CJ. Internal hydrogen effects on tensile properties of iron and Ni Base superalloys. Metall Trans A 1990;21:365 72.
[8] Fournier L, Delafosse D, Magnin T. Cathodic hydrogen embrittlement in alloy 718. Mater Sci Eng A 1999;269:111 9.
[9] Hicks PD, Altstetter CJ. Hydrogen enhanced cracking of superalloys. Metall Trans A 1992;23:237 49.
[10] Demetriou V, Robson JD, Preuss M, Morana R. Study of the effect of hydrogen charging on the tensile properties and microstructure of four variant heat treatments of nickel alloy 718. Int J Hydrogen Energy 2017. http://dx.doi.org/10.1016/j.ijhydene.2017.02.149. ISSN 0360 3199.
[11] Rezende MC, Araujo LS, Gabriel SB, dos Santo DS, de Almeida LH. Hydrogen embrittlement in nickel based superalloy 718: relationship between $\gamma' + \gamma''$ precipitation and the fracture mode. Int J Hydrogen Energy 2015;40:17075 83.
[12] Fukuyama S, Yokogawa K. Effect of heat treatments on hydrogen environment embrittlement of alloy 718. In: Superalloys 718, 625, 706 and various derivatives, Pittsburgh; 1994. p. 807 16.
[13] Wei W. The effect of hydrogen on the high temperature mechanical properties of in 718. In: Superalloys 718, 625, 706 and various derivatives, Pittsburgh; 1997. p. 705 14.
[14] Liu L, Zhai C, Lu C, Ding W, Hirose A, Kobayashi KF. Study of the effect of δ phase on hydrogen embrittlement of Inconel 718 by notch tensile tests. Corr Sci 2005;47:355 67.
[15] Sjoberg G, Cornu D. Hydrogen embrittlement of cast alloy 718 effects of homogeneization, grains size and δ phase. In: Superalloys 718, 625, 706 and Various Derivatives, Pittsburgh; 2001. p. 679 90.
[16] Liu L, Tanaka K, Hirose A, Kobayashi KF. Effects of precipitation phases on the hydrogen embrittlement sensitivity of Inconel 718. Sci Tech Adv Mater 2002;3:335 44.
[17] Pound BG. The effect of aging on hydrogen trapping in precipitation hardened alloys. Corr Sci 2000;42:1941 56.
[18] Robertson WM. Hydrogen permeation and diffusion in inconel 718 and incoloy 903. Metall Trans A 1977;8:1709 12.
[19] Galliano F, Andrieu E, Blanc C, Cloué JM, Connetable D, Odemer G. Effect of trapping and temperature on the hydrogen embrittlement susceptibility of alloy 718. Mat Sci Eng A 2014;611:370 82.
[20] Larignon C, Alexis J, Andrieu E, Odemer G, Blanc C. The contribution of hydrogen to the corrosion of 2024 aluminium alloy exposed to thermal and environmental cycling in chloride media. Corr Sci 2013;69:211 20.
[21] Clavel M, Pineau A. Frequency and wave form effects on the fatigue crack growth behavior of alloy 718 at 298 K and 823 K. Metall Trans A 1978;9:471 80.
[22] Tarzimoghadam Z, Ponge D, Klower J, Raabe D. Hydrogen assisted failure in Ni based superalloy 718 studied under in situ hydrogen charging: the role of localized deformation in crack propagation. Acta Mater 2017;128:367 74.
[23] Young GA, Scully JR. Evidence that carbide precipitation produces hydrogen traps in Ni 17Cr 8Fe alloys. Scr Mat 1997;36:713 9.
[24] Tanguy D, Wang Y, Connetable D. Stability of vacancy hydrogen clusters in nickel from first principles calculations. Acta Mater 2014;78:135 43.
[25] Li S, Li Y, Lo Y C, Neeraje T, Srinivasane R, Dinga X, et al. The interaction of dislocations and hydrogen vacancy complexes and its importance for deformation induced proto nano voids formation in α Fe. Int J Plast 2015;74:174 91.
[26] Zhu Y, Li Z, Huang M, Fan H. Study on interactions of an edge dislocation with vacancy H complex by atomistic modelling. Int J Plast 2017;92:31 44.
[27] Lawrence SK, Yagodzinskyy Y, Hänninen H, Korhonen E, Tuomisto F, Harris ZD, et al. Effects of grain size and deformation temperature on hydrogen enhanced vacancy formation in Ni alloys. Acta Mater 2017;128:218 26.
[28] Connetable D, Galliano F, Odemer G, Blanc C, Andrieu E. DFT study of the solubility of hydrogen and carbon in Ni_3Nb DO_a and Ni_3Nb DO_{22} systems. J Alloys Compd 2014;610:347 51.
[29] Tarzimoghadam Z, Rohwerder M, Merzlikin SV, Bashir A, Yedra L, Eswara S, et al. Multi scale and spatially resolved hydrogen mapping in a Ni Nb model alloy reveals the role of the δ phase in hydrogen embrittlement of alloy 718. Acta Mater 2016;109:69 81.
[30] Ferreira PJ, Robertson IM, Birnbaum HK. Hydrogen effects on the interaction between dislocations. Acta Mater 1998;46:1749 57.
[31] Moody NR, Perra MW, Robinson SL. Hydrogen induced cracking in an iron based superalloy. In: Moody NR, Thompson AW, editors. Hydrogen effects in material behavior; 1990. p. 625 34.
[32] Robinson SL, Somerday BP, Moody NR. Hydrogen embrittlement of stainless steel. In: Proc. of the 11th international conference on fracture, Turin, Italy; 2005. p. 672.